Time-resolved ellipticity gating of high-order harmonic emission

Lopez, Rodrigo; Mauritsson, Johan; Johnsson, Per; L'Huillier, Anne; Tcherbakoff, O.; Zair, A.; Mevel, E.; Constant, E

Published in:
Physical Review A

DOI:
10.1103/PhysRevA.69.053811

2004

Time-resolved ellipticity gating of high-order harmonic emission

R. López-Martens, J. Mauritsson, P. Johnsson, and A. L'Huillier
Department of Physics, Lund Institute of Technology, P. O. Box 118, S-22100 Lund, Sweden

O. Tcherbakoff, A. Zaïr, E. Mével, and E. Constant
CELIA, Université Bordeaux 1, 351 Cours de la Libération, 33405 Talence, France
(Received 11 September 2003; published 17 May 2004)

We present time-resolved cross-correlation measurements of extreme ultraviolet (xuv) pulses generated as high-order harmonics of intense 35 fs pulses, using a short (12 fs) probe pulse. We modulate the ellipticity of the laser driving the generation process such that the polarization is linear for short times around the temporal peak of the pulse. Since harmonic generation is strongly suppressed for very small amounts of driving laser ellipticity, the emission of xuv radiation can therefore be confined to times much shorter than the laser pulse duration. In addition, our setup allows us to continuously confine the xuv emission as well as to determine its frequency sweep during the pulse.

DOI: 10.1103/PhysRevA.69.053811 PACS number(s): 42.65.Ky, 32.80.Rm, 42.65.Re

Coherent attosecond light bursts produced during high-harmonic emission of atoms irradiated by intense femtosecond lasers bear the promise of being able to probe inner-shell electronic motion in atoms with unprecedented resolution [1]. The discrete nature and broad envelope spectrum of high-harmonic emission implies that appropriate phase locking of different harmonics can result in a train of pulses of attosecond duration [2]. Such early predictions are now strongly supported by recent experimental evidence indicating that harmonic emission from a macroscopic medium of atoms effectively consists of a train of attosecond pulses separated by one-half of the fundamental laser period [3,4].

The isolation of a single attosecond pulse from this train remains, however, a major physical challenge. Nevertheless, different strategies can be devised from our theoretical understanding of high-order harmonic generation, illustrated by a simple semiclassical picture [5,6]. In this picture, the electron initially released into the continuum and accelerated away from the parent ion in the direction of the linearly polarized driving laser field can return to the vicinity of the core and recombine every time the field reverses during an optical cycle of the laser. This results in successive bursts of extreme ultraviolet (xuv) radiation which are produced up to a cutoff frequency dependent on the intensity of the field. So far, the only successful scheme for isolating a single attosecond light burst is one that relies on the use of phase-stabilized linearly polarized few-cycle laser pulses together with spectral selection of the highest cutoff harmonics, for which the generation is naturally confined to a fraction of the laser oscillation period at the peak of the pulse [7,8]. Alternative schemes for single attosecond pulse generation, exploiting the acute sensitivity of harmonic generation efficiency to the ellipticity of the driving laser field [9], have been proposed. These are based on the temporal tailoring of the driving laser ellipticity in order to confine harmonic emission in the plateau region of the spectrum to a single xuv burst on a time scale less than a period of the laser field. Theoretical calculations [10–13] predict the formation of a single attosecond pulse (of duration of the order of 200 as) if short (10–15 fs) driving pulses are used.

Experimental attempts to demonstrate this technique, all performed in the spectral domain, reveal modulations in the harmonic spectrum which are consistent with a temporal confinement of the xuv emission but cannot be considered as direct proof [14–16]. To the best of our knowledge, no direct time-resolved measurement of such a confinement has yet been reported.

In this article, we show that by modulating in time the polarization of a 815 nm 35 fs pulse from a titanium sapphire laser, we can temporally confine the emission of plateau harmonics (13 to 21) generated in argon. Moreover, we can continuously tune the duration of the xuv pulses just by varying the segment of the driving pulse for which the polarization is linear and harmonic generation occurs efficiently. The xuv pulses thus generated in argon are characterized by cross correlation with an ultrashort (12 fs) ir probe pulse [17]. The cross-correlation signal is taken as the first order sideband appearing in the photoelectron spectrum of argon, corresponding to absorption of an xuv photon together with absorption or emission of one probe photon. By delaying one pulse with respect to the other, we can retrieve the time-frequency distribution of the xuv pulse: the duration can be inferred from the delay-dependent intensity of the sidebands [18,19], while the evolution of the instantaneous sideband energy can provide a measure of the linear chirp rate of the harmonic [20,21].

As illustrated in Fig. 1, the technique used to temporally modulate the ellipticity of the laser consists in transmitting the $\tau_0 = 35$ fs driving pulses through two quarter-wave plates of quartz [22]. The first quarter-wave plate (multiple order) splits the incoming linearly polarized pulse into an ordinary and an extraordinary pulse with crossed polarization. The group velocity difference between the two pulses leads to a delay through the 1.05 mm thick plate approximately equal to the pulse duration τ_0. When the optical axis of the first plate is oriented at $\alpha = 45°$ from the direction of incident laser polarization, a pulse is produced which is circularly polarized at the temporal center, when the two perpendicular fields have the same amplitude, and linear at both the leading

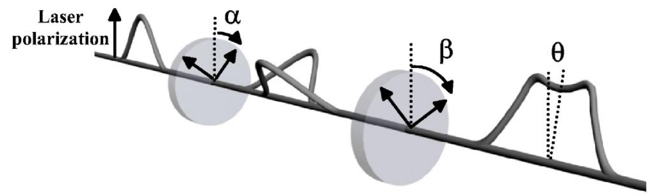

FIG. 1. Double quarter-wave plate arrangement used to temporally modulate the ellipticity of the driving laser pulse. θ is the angle between the major axis of the polarization ellipse of the resulting ellipticity modulated pulse and the incident direction of laser polarization.

and trailing edges. Transmission of this pulse through the second (zero-order) quarter-wave plate, with the optical axis oriented at $\beta=0°$ from the original direction of driving laser polarization, results in a pulse with a polarization that sweeps from circular through linear back to circular. Assuming an incident Gaussian shaped pulse of 35 fs duration [full width at half maximum (FWHM)], the temporal profile of the ellipticity modulated pulse is close to a flat top with 70 fs duration (FWHM), as shown by the dotted line in Fig. 2(a). The degree of ellipticity of the pulse strongly varies between $\varepsilon=1$ (circular polarization) at the wings to $\epsilon=0$ (linear polarization) at the center. The major axis of the ellipse described by the tip of the electric field vector is fixed during the pulse, oriented at $\theta=-45°$ from the initial laser polarization. More theoretical details on the role of the two plates can be found in [13]. The convolution of this ellipticity dependence with the sensitivity of harmonic generation to laser ellipticity, obtained from previous measurements [9], leads to the narrow temporal gate shown by the solid line, of 7 fs duration (FWHM). Changing the angle β allows us to continuously vary the width of the gate, as shown by the dashed line in Fig. 2(b). When $\beta=45°$, the polarization is always linear and the gate width is then the (70 fs) FWHM of the driving pulse. Except when $\beta=0$ or 90°, the major axis of the polarization ellipse rotates during the pulse, between θ_{min} and θ_{max} over the gate FWHM, as indicated by the solid lines in Fig. 2(b).

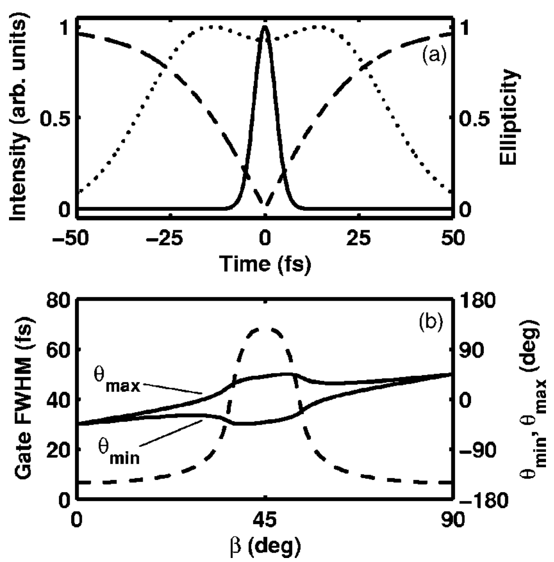

FIG. 2. (a) Dotted line: laser pulse envelope. Dashed line: time-dependent laser ellipticity. Solid line: temporal profile of the ellipticity gate obtained for $\beta=0°$. (b) Dashed line: temporal FWHM of the ellipticity gate. Solid lines: total angle of rotation swept by the laser polarization vector during this time calculated as a function of angle β.

The experimental setup used to measure the time-frequency distribution of harmonic pulses has been described elsewhere [20,21]. Our 1 kHz laser system produces 35 fs pulses centered at 815 nm with a total output energy of 2 mJ. A 1 mJ fraction is sent into an argon-filled hollow fiber. After compression with chirped mirrors, 0.5 mJ, 12 fs probe pulses are obtained. The remainder of the laser beam is routed through a variable delay line and then propagated through the double quartz plate arrangement in order to obtain driving laser pulses with the desired ellipticity modulation. These are finally focused by a $f=+50$ cm spherical mirror into a 3 mm windowless cell (filled with 30 mbar of argon) where the harmonics are generated. Care is taken in order to compensate any material dispersion before the harmonic generation cell. The generated time-gated harmonics are passed through a 200 nm thick aluminum filter to eliminate any residual driving infrared light. The harmonic generation point source is imaged downstream by a $f=+20$ cm normal incidence gold spherical mirror into the sensitive region of a magnetic bottle electron spectrometer (MBES), filled with a 1×10^{-4} mbar background pressure of argon. The collimated probe beam and the weakly diverging xuv beam are focused inside the MBES in a noncollinear fashion with the probe beam polarization pointing toward the direction of electron detection. The 2° angle between the two beams in the interaction region limits our overall temporal resolution to about 15 fs. Because both xuv and probe beams are overlapped using the same focusing optic, the difference in divergence between the two ensures that the xuv beam experiences a constant probe intensity throughout the interaction region.

Typical photoelectron spectra generated in the presence of the harmonic pulses consist of a comb of regularly spaced peaks corresponding to photoionization of argon induced by the individual harmonics of the plateau ranging from 13 to 21. The observation of higher harmonics is limited by the reflectivity of the gold mirror used in the MBES. When pump and probe pulses overlap in time and space, sidebands appear at intermediate photoelectron energies due to additional absorption or emission of one driving laser photon. The probe beam is attenuated by means of an external aperture in order to minimize the absorption of more than one ir photon by the ionizing atom. Figure 3 shows experimental data obtained under these conditions for sideband 18, labeled by the equivalent number of ir photons absorbed by the atom, and therefore corresponding to either absorption of the 17th harmonic plus one ir photon or absorption of the 19th harmonic minus one ir photon. The electron signal is plotted as a function of energy and time delay for $\beta=45°$ (large gate), $\beta=22°$ (intermediate gate), and $\beta=0°$ (narrow gate). As β decreases, the xuv emission signal clearly becomes confined to shorter time delays.

The temporal sideband intensity profiles, obtained by energy-integrating the electron signal, are plotted in Fig. 4 for the large and narrow gate cases, as well as for the case

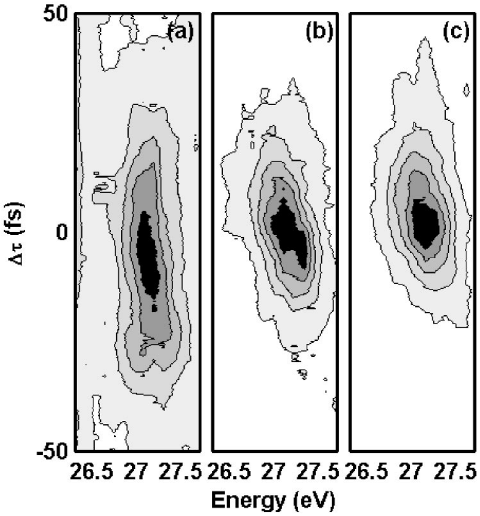

FIG. 3. Photoelectron signal obtained in Ar as a function of energy and time delay corresponding to sideband 18, generated from harmonics 17 and 19, for different angles on the second quarter-wave plate: (a) $\beta=45°$ (large gate), (b) $\beta=22°$ (intermediate gate), and (c) $\beta=0°$ (narrow gate).

when the ellipticity of the driving laser is not modulated ($\alpha=0°$, $\beta=0°$). In the absence of ellipticity modulation of the driving pulse, the sideband temporal profile is shifted toward positive time delays, indicating that the incident laser polarization is oriented along the slow axis of the first quarter-wave plate. The fact that this shift is very close to $\tau_0/2$ implies that the driving pulse experiences very little depletion during the harmonic generation process and that its peak intensity is below the ionization saturation intensity for argon. The temporal FWHM of the sideband profiles are 50 fs in the large gate configuration, 38 fs without any gate, and 22 fs in the narrow gate situation. The strong ellipticity modulation in the narrow gate case clearly leads to a significant shortening of duration of xuv emission.

In the absence of any ellipticity modulation of the driving pulse, a simple Gaussian deconvolution of the probe pulse duration from the sideband intensity profile yields an xuv

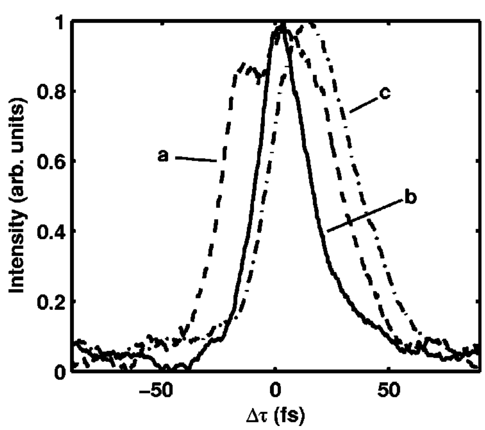

FIG. 4. Temporal intensity of sideband 18, generated from harmonics 17 and 19, measured for different ellipticity gate configurations: (a) large gate ($\alpha=45°$, $\beta=45°$), (b) narrow gate ($\alpha=45°$, $\beta=0°$), and (c) no gate ($\alpha=0°$, $\beta=0°$).

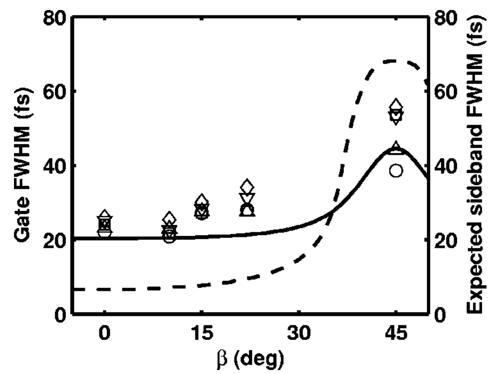

FIG. 5. Dashed line: calculated gate widths. Solid line: expected sideband widths after accounting for the generation and detection efficiency and for the temporal resolution of the setup. Experimental results are presented for different sideband orders: (○) 14, (△) 16, (□) 18, (▽) 20, (◇) 22.

pulse duration of 36 fs. In order to extract the confined xuv pulse durations, however, we have to account for the effect of the variation of the xuv polarization vector during the pulse on the two-photon ionization efficiency. From previous experimental studies [23], we know that the sideband intensity varies approximately as $P_{SB}(\theta)\approx 1-0.6\sin^2\theta$, θ being the relative angle between the xuv polarization vector and that of the probe field. In our experimental setup, the polarization vector of the probe field coincides with that of the fundamental laser field prior to the double quarter-wave plate arrangement as well as with the time-of-flight direction of the MBES. In addition, we observe that the collection efficiency of our MBES decreases by approximately 50% when the polarization vector of the electromagnetic field responsible for the ionization is at 45° from the direction of the time of flight. The harmonic pulse durations can be estimated by taking into account these effects and then by using a simple Gaussian deconvolution procedure accounting for the finite duration of the probe pulse. In the large gate configuration, this deconvolution procedure leads to pulse duration actually larger than the measured 50 fs width, almost equal to the 70 fs gate width. In the narrow gate case, the major axis of the polarization ellipse does not turn (see Fig. 2) and a straightforward deconvolution of the data leads to an xuv pulse duration of 18 fs, which is very close to the 15 fs maximum temporal resolution afforded by the noncollinear beam geometry used in this work.

Figure 5 compares the measured sideband temporal widths (symbols) with the expected ones (solid line), based on the theoretically calculated gate widths (dashed line), but accounting for the θ-dependent detection efficiency as well as for the temporal resolution of the experiment. The agreement between the experimental results and the expected sideband widths is quite satisfactory, and independent of the sideband number (from 14 to 20). This indicates that the duration of xuv emission is indeed limited by the ellipticity gate, rather than the harmonic generation process. These results also show that, just by rotating the second plate in the setup, the duration of xuv emission can be continuously confined right down to the limit of temporal resolution afforded by the experiment, beyond which no further confinement can be resolved.

The other significant feature of the raw data presented in Fig. 3 is the concomitant change in the rate of frequency chirp of the xuv emission, as inferred by the change in the tilt in energy of the sidebands, observed as the xuv emission is confined in time. Even for linearly polarized fundamental driving pulses, the harmonic pulses are in general chirped, due to ionization of the nonlinear medium, the dipole phase variation, or some residual fundamental frequency variation [20]. The ellipticity modulation of the fundamental pulse might also lead to additional chirp on the harmonics. For example, any increase of the spectral bandwidth due to the confinement will lead to a change in the chirp rates. The frequency chirp rate of the xuv emission which can be deduced from the experimentally observed sideband energy tilt as well as the measured pulse duration is negative and is found to increase in value as β decreases, with a maximum around 10°, and to decrease again, in qualitative agreement with recent theoretical predictions [13]. The maximum negative chirp observed, e.g., for the 19th harmonic is 18 meV/fs. This indicates the possibility of recompressing the xuv pulse duration to values even shorter than those imposed by the ellipticity gate.

In conclusion, we have shown that by temporally modulating the driving laser, the xuv emission can be confined to a time interval which is at least shorter than half the one measured when the driving ellipticity is not modulated. This confinement factor does not represent a limitation of the technique but rather of the cross-correlation measurement, which could be improved by using a collinear geometry and shorter probe pulses. The xuv pulse shortening reported in this work represents the first unequivocal proof of confinement of plateau harmonics by temporally gating the driving laser ellipticity, thereby offering encouraging prospects for its application to shorter pulses.

We acknowledge the support of the European Community (under Contracts No. HPRI-CT-1999-00041 and No. HPRN-CT-2000-00133, ATTO) the Swedish Science Council, the Knut and Alice Wallenberg Foundation, and the European Science Foundation.

[1] M. Drescher *et al.*, Nature (London) **419**, 803 (2002).
[2] G. Farkas and C. Tóth, Phys. Lett. A **168**, 447 (1992); S. E. Harris, J. J. Macklin, and T. W. Hänsch, Opt. Commun. **100**, 487 (1993).
[3] P. M. Paul *et al.*, Science **292**, 902 (2001).
[4] Y. Mairesse *et al.*, Science **302**, 1540 (2003).
[5] P. B. Corkum, Phys. Rev. Lett. **71**, 1994 (1993).
[6] K. J. Schafer, B. Yang, L. F. DiMauro, and K. C. Kulander, Phys. Rev. Lett. **70**, 1599 (1993).
[7] M. Hentschel *et al.*, Nature (London) **414**, 509 (2001).
[8] R. Kienberger *et al.*, Science **297**, 1194 (2002).
[9] P. Dietrich, N. H. Burnett, M. Ivanov, and P. B. Corkum, Phys. Rev. A **50**, R3585 (1995); K. S. Budil *et al.*, *ibid.* **48**, R3437 (1993); Y. Liang *et al.*, J. Phys. B **27**, 1296 (1994).
[10] P. B. Corkum, N. H. Burnett, and M. Y. Ivanov, Opt. Lett. **19**, 1870 (1994).
[11] V. T. Platonenko and V. V. Strelkov, J. Opt. Soc. Am. B **16**, 435 (1999).
[12] P. Antoine *et al.*, Phys. Rev. A **56**, 4960 (1997).
[13] V. Strelkov *et al.*, Appl. Phys. B: Lasers Opt. (to be published).
[14] C. Altucci *et al.*, Phys. Rev. A **58**, 3934 (1998).
[15] O. Tcherbakoff *et al.*, Phys. Rev. A **68**, 043804 (2003).
[16] M. Kovacev *et al.*, Eur. Phys. J. D **26**, 79 (2003).
[17] M. Nisoli *et al.*, Opt. Lett. **22**, 522 (1997).
[18] T. E. Glover, R. W. Schoenlein, A. H. Chin, and C. V. Shank, Phys. Rev. Lett. **76**, 2468 (1996).
[19] A. Bouhal *et al.*, Phys. Rev. A **58**, 389 (1998).
[20] J. Norin *et al.*, Phys. Rev. Lett. **88**, 193901 (2002).
[21] R. López-Martens *et al.*, Eur. Phys. J. D **26**, 105 (2003).
[22] D. Y. Smith, E. Shiles, and M. Inokuti, in *Handbook of Optical Constants of Solids*, edited by E. D. Palik (Academic, Orlando, FL, 1985).
[23] P. O'Keefe *et al.*, Phys. Rev. A (to be published).